

# Dielectric relaxation, Ionic conduction and Complex impedance studies on $\text{NaNO}_3$ fast ion conductor

T. Vijay kumar<sup>1</sup>, A. Sadananda Chary<sup>2</sup>, Suresh Bhardwaj<sup>3</sup>, A. M. Awasthi<sup>3</sup>, S. Narender Reddy<sup>4,\*</sup>

<sup>1</sup>Department of Physics, Arjun College of Technology and Sciences, JNTUH, India

<sup>2</sup>Dept. of Physics, University College of Science, Osmania University, Hyderabad, India

<sup>3</sup>Thermodynamics Lab, UGC DAE Consortium, Indore, India

<sup>4</sup>Dept. of Physics, University College of Engineering, Osmania University, Hyd, India

## Email address:

physicistvijay@gmail.com(T. Vijay Kumar), snreddy\_sattineni2000@yahoo.com(S. Narender Reddy)

## To cite this article:

T. Vijay kumar, A. Sadananda Chary, Suresh Bhardwaj, A. M. Awasthi, S. Narender Reddy. Dielectric Relaxation, Ionic Conduction and Complex Impedance Studies on  $\text{NaNO}_3$  Fast Ion Conductor. *International Journal of Materials Science and Applications*. Vol. 2, No. 6, 2013, pp. 173-178. doi: 10.11648/j.ijmsa.20130206.12

**Abstract:** AC conductivity, dielectric constant, loss and electric modulus of Sodium nitrate system have been studied in the frequency range from 1Hz to 10MHz and in the temperature range from 303 K to 563 K by employing impedance spectroscopy. The frequency dependent ac conductivity follows Jonscher's universal power law. Dimensionless frequency exponent (n), dispersion parameter (A) are determined. The change over frequency independent conductivity to frequency dependent conductivity at all temperatures shows the relaxation mechanism. The variation of real part of dielectric constant with frequency shows strong dispersion at low frequencies and saturation at high frequencies. The presence of peaks in the frequency plots of dielectric loss, imaginary parts of impedance and modulus are attributed to the relaxation processes. It is also confirmed by the temperature dependence study of real part of dielectric constant. The activation energy from relaxation processes and conductivity has been evaluated.

**Keywords:** Solid Electrolyte, Fast Ion Conductor, Relaxation, Ac Conductivity

## 1. Introduction

Study of Solid State Ionics, which deals with the fast ion transport in solids, has attracted a great deal of interest in material scientists for the last few decades. Solid electrolytes or superionic materials possess exceptionally high ionic conductivity at ambient temperatures which have numerous technological applications in a variety of solid state electrochemical devices such as solid-state batteries, super capacitors, electro-chromic displays, sensors, electrochemical solar cells etc [1-2]. Recently the high energy density  $\text{Na}^+$  ion conducting batteries have been developed by Brain et al because of their light weight and high electrochemical potential [3]. The discovery of sodium ion transport in  $\beta'$  and  $\beta''$  alumina [4] has motivated the researchers on other  $\text{Na}^+$  fast ion conductors. Sodium nitrate, which is considered as an excellent  $\text{Na}^+$  ion conductor, exhibits high conductivity in the order of  $10^{-4}$  S/cm. The crystal structure of sodium nitrate is rhombohedral calcite structure with a space group  $R3c$ , with two molecules in the unit cell and has an orientational

disorder of nitrate ion at 548 K [5]. The earlier conductivity studies show that the charge transport in sodium nitrate is mainly due to cationic Frenkel defects [6]. Hence, the present work is directed towards investigation of sodium nitrate system.

Complex impedance spectroscopy is a very useful technique to investigate the microstructure and the electrical properties of solid materials and this has been extensively employed in Solid State Ionics, due to the following capabilities: i) to resolve grain boundary from

bulk electrical properties, ii) to estimate conductivity and dielectric constant and iii) to probe the electrical homogeneity [7]. The dielectrical properties such as impedance, dielectric constant, loss, ac conductivity and modulus are presented in order to correlate the conduction mechanism and relaxation phenomena.

## 2. Experimental

The single crystals of  $\text{NaNO}_3$  were grown by slow evaporation technique by dissolving the powder (99.9%

purity) in double distilled water. These crystals were ground in an agate mortar and this process of grinding was continued for several hours. The fine powder so obtained was sieved and then pressed as pellets at a pressure of about 5 tonnes/sq.m by using hydraulic press. Pellets of 12mm diameter and 1-2 mm thickness were sintered at 200°C for 24 h. After polishing the surfaces, silver paste was applied for good electrical contact and mounted between the two electrodes of the sample holder. The impedance measurements were carried out in the frequency range 1Hz-10MHz over the temperature range of 303 K – 563 K in the intervals of 5 K, by employing Novo control Alpha-A, a high performance frequency analyzer at UGC-DAE Consortium for Scientific Research, Indore.

### 3. Results and Discussion

#### 3.1. X-Ray Diffraction

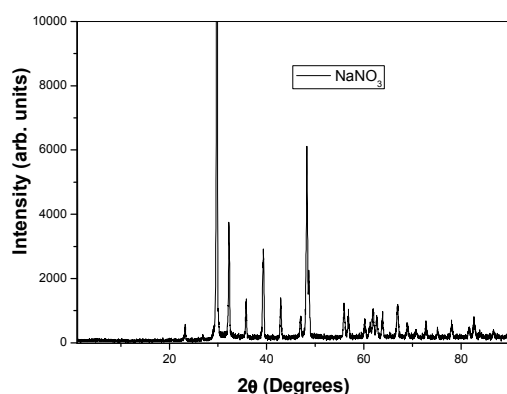


Fig.1: X-ray diffraction pattern of the pure  $\text{NaNO}_3$

X-ray powder diffraction pattern of the pure  $\text{NaNO}_3$  solid electrolyte, recorded at room temperature by Regaku miniflex diffractometer, is shown in Fig.1. The presence of distinct, sharp and high intense peaks confirms the crystalline nature of  $\text{NaNO}_3$ . The Lattice parameter of  $\text{NaNO}_3$  (rhombohedral) structure is calculated using diffraction data i.e.  $6.324\text{\AA}$ , which is in good agreement with the literature value [8].

#### 3.2. Fourier Transform Infrared Spectrum

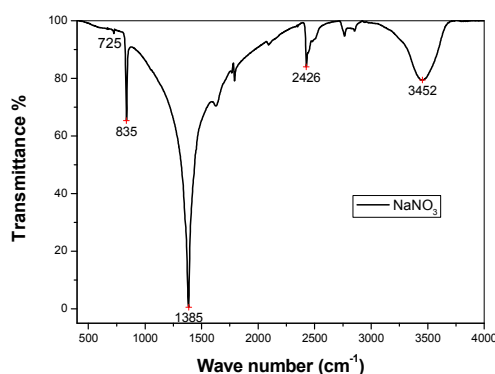


Fig.2: FTIR spectrum of pure  $\text{NaNO}_3$

The FTIR transmittance spectrum of  $\text{NaNO}_3$  recorded in the wave number range from 400 to 4000  $\text{cm}^{-1}$  confirms the presence of different inorganic materials and is shown in Fig.2. In pure  $\text{NaNO}_3$ , the sharp peaks at 835  $\text{cm}^{-1}$ , 1385  $\text{cm}^{-1}$  and 2426  $\text{cm}^{-1}$  were observed. These values are in good agreement with the earlier reported values on same system by Foil A Miller *et al* [9]. The sharp peak observed at 835  $\text{cm}^{-1}$  is due to the vibration of N in and out of  $\text{NO}_3$  plane and the strongest absorption at 1385  $\text{cm}^{-1}$  due to asymmetric  $\text{NO}_3$  stretch which confirms the presence of nitrate. The weak absorption which is observed at 725  $\text{cm}^{-1}$  gives the doubly degenerate O-N-O bending [10].

#### 3.3. Dielectric Study

The study of the dielectric properties is essential because it gives valuable information about loss of energy, conduction mechanism and relaxation processes. Fig.3 shows the frequency dependence of real part ( $\epsilon'$ ) and imaginary part ( $\epsilon''$ ) of the dielectric constant for  $\text{NaNO}_3$  at various temperatures. It is observed that the values of real and imaginary parts of the dielectric constant decrease with frequency and attain a constant limiting value. This can be attributed to free dipoles oscillating in an alternating electric field. At very low frequencies ( $f \ll 1/\tau$ ,  $\tau$  is the relaxation time), dipoles follow the electric field and at very high frequencies ( $f \gg 1/\tau$ ), dipoles can no longer follow the field. As the frequency increases ( $f < 1/\tau$ ), dipoles begin to lag behind the field and when the frequency reaches the characteristic frequency ( $f = 1/\tau$ ), the dielectric constant falls steeply [11-12]. At low frequencies, the dispersion of real and imaginary parts of dielectric constant is due to space charge polarization which is observed for all the temperatures [13]. The  $\log(\epsilon'')$  vs.  $\log(f)$  plot at different temperatures is shown in the inset of Fig.3. The slope of the straight line lying between  $-0.8$  and  $-0.98$  which is nearly equal to  $-1$  indicates that the contribution from dc conduction is predominant in the system from 423 K to 563K [14-15]. The deviation of the slope from unity could be due to space charge effects at low frequencies.

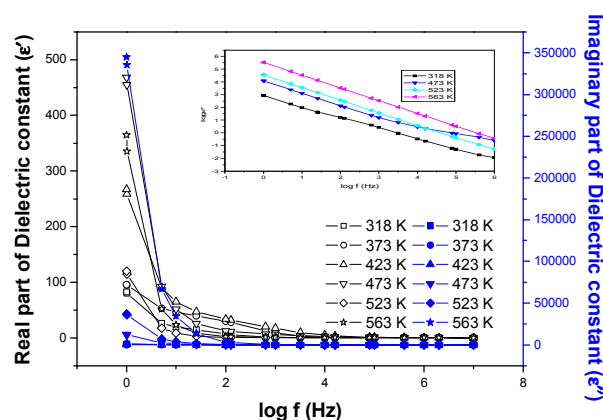


Fig.3: Variation of real and imaginary parts of dielectric constant with frequency at different temperatures. Inset Fig. shows the  $\log(\epsilon'')$  vs.  $\log(f)$  plot at different temperatures.

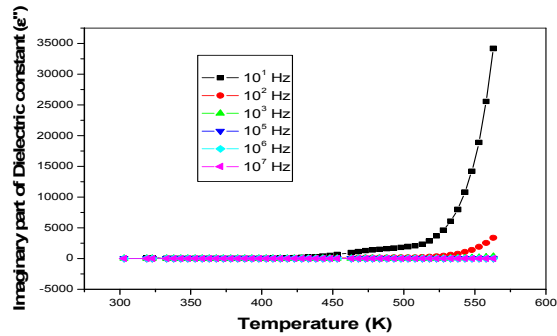


Fig.4: Variation of imaginary part of dielectric constant with temperature at different frequency

It can be seen from the Fig.4 that there is a gradual increase in  $\epsilon''$  at low temperatures which rises sharply from 550K onwards because of the thermally generated defects [16]. The temperature dependence of  $\epsilon'$  for 100Hz, 1 KHz, 100 KHz and 1000 KHz frequencies is displayed in Fig.5. The broad peaks over a wide temperature range from 403 K – 473 K observed for all frequencies shift towards high temperatures with frequency, this indicates the existence of dielectric relaxation [17].

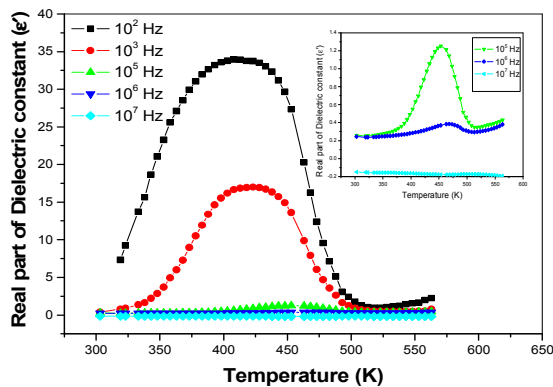


Fig.5: Variation of real part of dielectric constant with temperature at different frequencies. Inset Fig. shows the variation of real part of dielectric constant at high frequencies.

Fig.6a depicts the variation of loss tangent with frequency at different temperatures. The plots corresponding to low temperatures are incorporated in Fig. 6b. It can be seen that the  $\tan \delta$  peaks shift towards high frequencies with rise in temperature which confirms dielectric relaxation phenomenon. The peak frequency,  $f_{\tan}$ , as a function of temperature, which is shown in Fig.6c, follows the Arrhenius relation in both regions of temperature [18]. The activation energy is calculated from the slope of the  $\log(f_{\tan})$  vs.  $1000/T$  plot to be 0.66 eV in the temperature range 403 K- 473 K and 1.17 eV in the temperature range 503 K- 563 K, which agrees with activation energy obtained from conductivity data in our earlier work [19]. The dielectric loss shows a maximum at low frequency end in the high temperature region because of thermally generated defects in the sample. The relatively large value of  $\tan \delta$  at these temperatures could be due to the contribution from conduction process in the system [20-21].

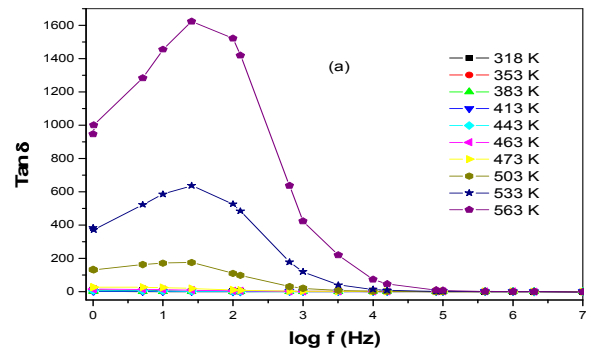


Fig.6a: Variation of loss tangent ( $\tan \delta$ ) with frequency at high temperatures

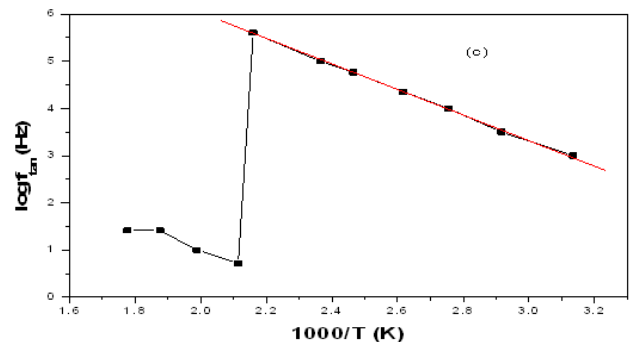
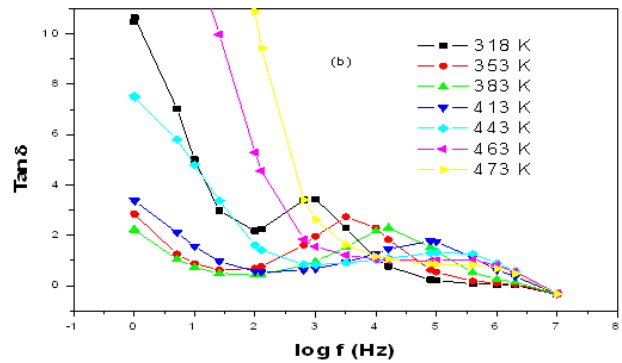
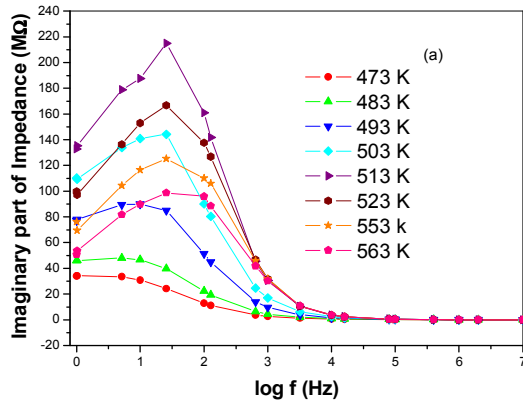


Fig.6: Variation of loss tangent ( $\tan \delta$ ) with frequency (b) at low temperatures and (c) shows  $1000/T$  vs.  $\log f_{\tan}$  plot

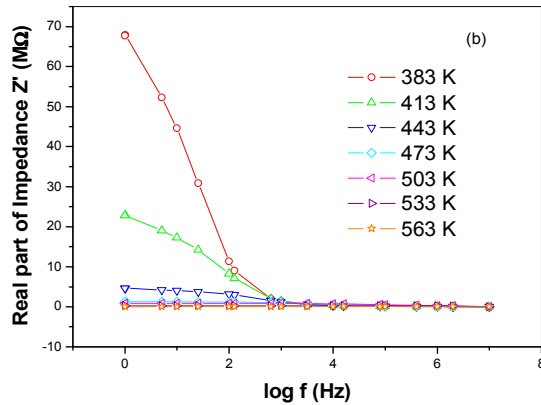
### 3.4. Impedance Analysis

Fig.7a shows the imaginary part of impedance  $Z''$  as a function of frequency at different temperatures. A broad peak, which can be seen at about 10Hz for 473K, is observed to shift towards higher frequencies as the temperature increases.  $Z''$  reaches to a constant value for all temperatures above 10 kHz. It suggests that the relaxation behavior is related to thermally activated processes. The peak frequency,  $f_{Z''}$ , as a function of temperature follows the Arrhenius relation. The activation energy 1.12 eV is calculated from the slope of the  $\log(f_{Z''})$  vs.  $1000/T$  plot, which agrees with activation energy obtained from dielectric loss studies.



**Fig. 7a:** Variation of imaginary part of impedance with frequency at different temperatures

The Fig. 7b shows the variation of real part of impedance ( $Z'$ ) with frequency for NaNO<sub>3</sub> at different temperatures. It is observed that the magnitude of  $Z'$  decreases with the increase of temperature indicates that there is an increase in conductivity. The value of  $Z'$  appears to be independent of frequency for all the temperatures indicating that there is an increase in the concentration of defects with the rise in temperature resulting in increase of conductivity in the system [22].



**Fig. 7b:** Variation of real part of impedance with frequency at different temperatures

### 3.5. AC Conductivity

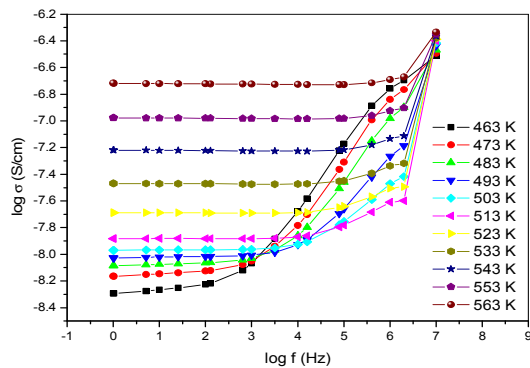


**Fig. 8:** Variation of ac conductivity with frequency at different temperatures.

The log-log plot of frequency versus ac conductivity at different temperatures is shown in Fig. 8. The ac conductivity is calculated from the dielectric data using the relation  $\sigma_{ac} = 2\pi f \epsilon' \epsilon_0 \tan \delta$  [11]. It can be observed that the ac conductivity increases with increasing frequency for all the temperatures. The ac conductivity is observed to be nearly independent at low frequencies followed by dispersion of the conductivity at higher frequencies. As the temperature increases, the frequency independent region increases and frequency dependent region decreases which can be attributed to the relaxation due to the onset of conduction processes [23]. The hopping frequency ( $f_h$ ), at which the conductivity relaxation begins to appear, is observed to shift towards the higher frequencies with rise in temperature. The observed frequency dependence of conductivity can be described by the Jonscher's universal power law [24-25] given as

$$\sigma_T = \sigma_0 + A f^n$$

Where  $\sigma_0$  is the frequency independent conductivity of the material,  $A$  is the dispersion parameter and  $n$  is the dimensionless frequency exponent, which is a measure of the degree of interaction with the values 0 and 1 for an ideal Debye dielectric dipolar-type and an ideal ionic-type crystal respectively. The typical values of  $n$ , between 0 and 1, represent ac conduction through hopping mechanism [24]. The frequency dependent conductivity ( $\sigma_{ac}$ ) data has been fitted by using Jonscher's universal power law. The value of  $n$  can be obtained from the slopes of the plots  $\log \sigma_{ac}$  vs.  $\log f$  and  $A$  from the intercept. Table 1 summarizes the fitted values of  $A$  and  $n$  at different temperatures.

**Table 1.** The values of  $n$ ,  $A$  and  $\sigma_0$  for different temperatures.

Temperature(K)	$n$	$A$ (S $\text{cm}^{-1}\text{S}^n$ )	$\sigma_0$ (S $\text{cm}^{-1}$ )
563	1.39	$4.53 \times 10^{-17}$	$1.91 \times 10^{-7}$
553	1.37	$6.48 \times 10^{-17}$	$1.06 \times 10^{-7}$
543	1.34	$1.17 \times 10^{-17}$	$6.05 \times 10^{-8}$
533	0.91	$4.10 \times 10^{-14}$	$3.39 \times 10^{-8}$
523	0.69	$7.21 \times 10^{-13}$	$2.06 \times 10^{-8}$
513	0.66	$1.11 \times 10^{-12}$	$1.31 \times 10^{-8}$
503	0.62	$3.84 \times 10^{-12}$	$1.08 \times 10^{-8}$
493	0.61	$8.51 \times 10^{-12}$	$9.44 \times 10^{-9}$
483	0.60	$2.23 \times 10^{-11}$	$8.29 \times 10^{-9}$
473	0.57	$4.50 \times 10^{-11}$	$7.14 \times 10^{-9}$
463	0.54	$8.50 \times 10^{-11}$	$5.33 \times 10^{-9}$
453	0.52	$1.23 \times 10^{-11}$	$3.32 \times 10^{-9}$
443	0.47	$3.15 \times 10^{-10}$	$1.93 \times 10^{-9}$

It can be seen from the Table 1 that  $n$  is less than one for temperatures below 543 K and greater than 1 for the temperature at and above 543 K. The latter category corresponds to long-range diffusion of ions [26-27]. The observed frequency vs. conductivity behavior is explained by using jump relaxation model [28-29], according to

which an ion jumps from a site to its neighbouring vacant site at low frequencies where as dispersion region is characterized by the random hopping of mobile ions and the conductivity is correlated to the forward-backward hopping of the ions leading to the long-range diffusion of ions at high frequency end[30-31]. The increase in ac conductivity could be attributed to the lowering of the activation barrier at higher frequencies as compared to that at lower frequencies [32].

### 3.6. Electric Modulus

As discussed above, the peaks in the dielectric, impedance and ac conductivity studies confirms the presence of a relaxation phenomenon in the system. In order to reconfirm the relaxation process in the sample the real and imaginary parts of moduli are calculated using the relations  $M' = \epsilon' / (\epsilon'^2 + \epsilon''^2)$  and  $M'' = \epsilon'' / (\epsilon'^2 + \epsilon''^2)$  since  $M^* = 1/\epsilon^*$ . The plot of the real part of the complex modulus with the frequency for different temperatures is shown in the Fig.9a. Dispersion is observed as frequency rises, and reaches to a maximum value at high frequencies ( $10^6$  Hz). It tends to zero at lower frequencies ( $10^3$  Hz and below) which indicates that the effect of electrode and electrolyte interface polarization has been minimized in the modulus spectrum which was observable in dielectric constant and loss [33-34].

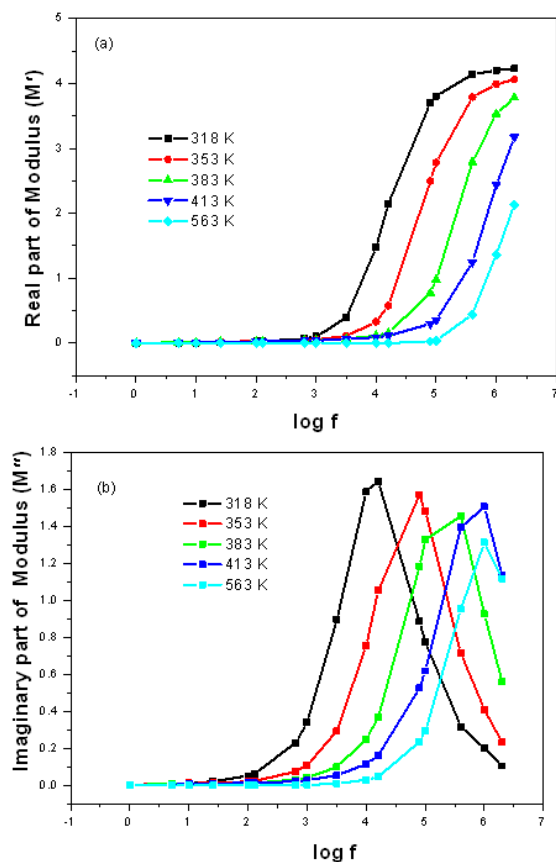


**Fig.9:** Variation of (a) imaginary part (b) real part of complex modulus with frequency at different temperatures .

The variation of the imaginary part of  $M^*$  with the frequency at different temperatures  $\text{NaNO}_3$  is shown in Fig.9b. It is clear from the figure that the modulus spectrum has a long horizontal line at the low frequency end and the broad peak is seen at high frequencies for all temperatures. The position of the peak shifts toward the higher frequency end as the temperature is raised upto 473 K. The peak frequency ( $f_M$ ) as a function of temperature follows the Arrhenius relation and the relaxation time ( $\tau_m$ ) can be calculated by using relation  $\omega_m \tau_m = 1$ , where  $\omega_m$  peak frequency at particular temperature. By fitting the plot  $1000/T$  vs.  $\log f_M$  the obtained activation energy is 0.62 eV in the temperature range 403 K- 473 K and 1.11 eV in the temperature range 503 K- 563 K, which is in good agreement with the obtained activation energy in the dielectric loss study.

## 4. Conclusion

The frequency dependent conductivity of  $\text{NaNO}_3$  at different temperatures has been analyzed using a Jonscher's power law and the evaluated values of frequency exponent suggest that an ion jumps from one site to other neighboring vacant site at low frequencies where as the dispersion in the high frequency region is characterized by long-range diffusion of ions. The dielectric, impedance, ac conductivity and modulus analyses showed the peaks, reveals the relaxation processes. The activation energies evaluated from dielectric, impedance, conductivity, modulus studies are in good agreement and these values confirm the transport in the present system is through hopping mechanism.

## References

- [1] S Chandra, "Superionic solids: Principles and Application s", Amsterdam, North-Holland, 1981.
- [2] P.G. Bruce, "Solid State Electrochemistry", Cambridge University Press, Cambridge, 1995.
- [3] Brian L. Ellis, Linda F. Nazar, "Sodium and sodium-ion energy storage batteries", Current Opinion in Solid State and Materials Science, vol. 16, pp.168-177,2012.
- [4] K.D. Kreuer., H. Kohler, J. Maier, in: T. Takahashi (Ed.), "High Conductivity Ionics Conductors: Recent Trends and Applications", World Scientific Publishing Co., Singapore, 1989.
- [5] Badr and Kamel, "Comparative study of structure changes with temperature in univalent and divalent ionic nitrate crystals", J. Phys. Chem. Solids, vol.41(10), pp.1127-1131, 1980.
- [6] C. Ramasastry, Y.V.G.S. Murti, "Electrical conduction in sodium nitrate crystals", Proc. Roy. Soc. A, vol. 305(1483), pp. 441-445, 1968.
- [7] Jin-Ha H., Mason T. O., Garboczi, "Electrical/dielectric properties of nano crystalline cerium oxide in nano phase and nanocomposite materials II", Materials Research



- Society, vol. 457, pp. 27-32, 1997.
- [8] Wyckoff, R.W.G., "The crystal structures of some carbonates of the calcite group", *Phys. Rev. Vol. 16*, pp. 149, 1920.
- [9] Foil A. Miller, Charles H, Wilkins," Infrared spectra and characteristic frequencies of Inorganic ions", Department of Research in Chemical Physics, Mellon Institute, Pittsburgh 13 Pa., vol. 24 (8), pp.1255-1256, 1952.
- [10] J. Greenberg, and L.J Hallgren, "Infrared absorption spectra of alkali metal nitrates and nitrites above and below the melting Point", *J.chem.Phys.* vol.33 (3), pp. 900-902, 1960.
- [11] Ved Prakash, S.N. Choudhary, T.P. Sinha, "Dielectric relaxation in complex perovskite oxide  $\text{BaCo}_{1/2}\text{W}_{1/2}\text{O}_3$ " *Physica B*, vol.403, pp.103-108, 2008.
- [12] Tripathi, R., Kumar, A., Bharti, Ch., Sinh, T. P. "Dielectric relaxation of ZnO Nanostructure Synthesized by Soft Chemical Method", *Current Applied Physics*, vol. 10 (2), pp. 676 – 681, 2010.
- [13] Sambasiva Rao K., Murali Krishna P., Madhava Prasad D., Joon-Hyung L., Jin-Soo K, "Electrical, Electromechanical and structural studies of Lead Potassium Samarium Niobat Ceramics", *Journal of Alloys and Compounds*, vol.464 (1 – 2) pp. 497 – 507, 2008.
- [14] Bharadwaja S S N, Krupanidhi S B, "Study of AC electrical properties in multigrain antiferroelectric lead zirconate thin films", *Thin Solid Films*, vol.391, pp.126, 2001.
- [15] M. Arous, I. Ben Amor, A. Kallel, Z. Fakhfakh, G. Perrier, " Crystallinity and dielectric relaxation in semi crystalline poly( ether ether ketone)", *J Physics and Chemistry of Solids*, vol. 68(7), pp. 1405-1414, 2008.
- [16] B. Tareev, *Phys. "Dielectric Materials"*. Mir Publication, Moscow, 1979.
- [17] A.M. Abo El Ata, M.A. Ahmed, "Dielectric and AC conductivity for  $\text{BaCo}_{2-x}\text{Cu}_x\text{Fe}_{16}\text{O}_{27}$  ferrites", *Journal of Magnetism and Magnetic Materials* vol.208(1-2), pp. 27-36, 2000.
- [18] Mohamad M. Ahmad, Koji Yamada and Tsutomu Okuda, "Ionic conduction and relaxation in  $\text{KSn}_2\text{F}_5$  fluoride ion conductor", *Physica B*, vol. 339(2-3), pp. 94-100, 2003.
- [19] M.V. Madhava Rao, S. Narender Reddy, A. Sadananda Chary, "DC ionic conductivity of  $\text{NaNO}_3$ - $\gamma$   $\text{Al}_2\text{O}_3$  composite solid electrolyte system", *Physica B*, vol. 362, pp.193-198, 2005.
- [20] R.J MacCallum, C.A. Vicent, "Polymer Electrolyte Reviews II", Elsevier Applied Science Publishers Ltd, London and Newyork, 1987.
- [21] A.Kyritsis, P.Pissis, J.Grammatikakis, "Dielectric relaxation spectroscopy in poly(hydroxyethyl acrylates)/water hydrogels " *J.Polym. Sci. Part B:Polym, Phys.*, vol. 33(12), pp. 1737-1750, 1995.
- [22] Amodini Mishra, S.N.Choudhary , K.Prasad , R.N.P.Choudhary, " Complex impedance spectroscopic studies of  $\text{Ba}(\text{Pr}_{1/2}\text{Ta}_{1/2})\text{O}_3$  ceramic", *Physica B*, vol. 406, pp. 3279-3284, 2011.
- [23] N.K. Karan, B. Natesan, R.S. Katiyar, "Structural and lithium ion transport studies in pyrophosphate glasses" *Solid State Ionics*, vol. 177(17-18), pp. 1429-1436, 2006.
- [24] A.K. Jonscher, "Analysis of the alternating current properties of ionic conductors" *J. Mater. Sci.*, vol.13(2), pp. 553-562,1978.
- [25] A.K. Jonscher, "The universal dielectric response" *Nature*, vol. 267(5613), pp. 673-679, 1977.
- [26] B. Louati, M. Garouri, K. Guidara, T. Mhiri, "AC electrical properties of the mixed crystal  $(\text{NH}_4)_3\text{H}(\text{SO}_4)_{1.42}(\text{SeO}_4)_{0.58}$ ", *J. Phys. Chem. Solids*, vol. 66(5), pp. 762-765, 2005.
- [27] R.H. Chen, Li-Fang Chen, Chih-Ta Chia, "impedance spectroscopic studies on congruent  $\text{LiNbO}_3$  single crystal " *J. Phys.: Condens. Matter*, vol.19, pp. 086225, 2007.
- [28] J.C. Dyre, Th.B. Schröder, "Ac hopping conduction at extreme disorder takes place on the percolating cluster", *Phys. Stat. Sol. B*, vol. 230, pp.5, 2002.
- [29] A.R. Kulkarni, P. Lunkenheimer, A. Loidl, "Scaling behaviour in the frequency dependent conductivity of mixed alkali glasses", *Solid State Ionics*, vol.112(1-2), pp. 69-74, 1998.
- [30] Le Meins J M, Bohnke O, Courbion G.; Ionic conductivity of crystalline and amorphous  $\text{Na}_3\text{Al}_2(\text{PO}_4)_2\text{F}_3$ , *Solid State Ionics*, vol.111(1-2). Pp.67-75, 1998.
- [31] S.H. Chung, K.R. Jeffrey, J.R. Stevens, L. Börjesson, "Dynamics of silver ions in  $(\text{AgI})_x-(\text{Ag}_2\text{O}-n\text{B}_2\text{O}_3)_{1-x}$  glasses: A  $^{109}\text{Ag}$  nuclear magnetic resonance study" *Phys. Rev. B*, vol. 41(10), pp. 6154-6164, 1990.
- [32] M.V. Madhava Rao, S. Narender Reddy, A. Sadananda Chary, K. Shahi, "Complex impedance analysis of  $\text{RbNO}_3$  and  $\text{RbNO}_3:\text{Al}_2\text{O}_3$  dispersed solid electrolyte systems", *Physica B*, vol. 364, pp. 306-310. 2005.
- [33] R.H. Chen, Yu-Chao Chen, C.S. Shern, T. Fukami, "Conductivity and dielectric relaxation phenomena in  $(\text{NH}_4)_2\text{SO}_4$  single crystal", *Solid State Ionics*, vol.180(4-5),pp. 356- 361,2009.
- [34] J.M. Bose, J.M. Reau, J. Senegas, M. Poulain, " $\text{F}^-$  ion conductivity and diffusion properties in  $\text{ZrF}_4$ -based fluoride glasses with various NaF concentrations ( $0 \leq x_{\text{NaF}} \leq 0.45$ )" *Solid State Ionics*, vol. 82(1-2), pp. 39-52, 1995.